ARID ZONE JOURNAL OF ENGINEERING, TECHNOLOGY & ENVIRONMENT
AZOJETE December 2024. Vol.20(4):790-812
Published by the Faculty of Engineering, University of Maiduguri, Maiduguri, Nigeria.
Print ISSN: 1596-2490, Electronic ISSN: 2545-5818
www.azojete.com.ng

ORIGINAL RESEARCH ARTICLE

DESIGN AND ANALYSIS OF FLIGHT PERFORMANCE OF A HYBRID ENERGY SOURCE FOR UNMANNED AERIAL VEHICLE

D. N.O. Eleazer[1], U. E. Uche[2*], M. Tajudeen[3] and I. M. B. Omiogbemi[2]

[1]Department of Aerospace Engineering, Faculty of Air Engineering Air Force Institute of Technology, Kaduna, Nigeria,
[2]Department of Mechanical Engineering, Air Force Institute of Technology, Kaduna, Nigeria,
[3]Department of Material and Metallurgical Engineering, Air Force Institute of Technology, Kaduna, Nigeria.
**Corresponding author's email address: eaumie@gmail.com*

ARTICLE INFORMATION

Submitted: 30 May, 2024
Revised: 29 June, 2024
Accepted: 08 July, 2024

Keywords:
Hydrogen
Fuel
Cell
Solar
Hybridization
Endurance
Range

ABSTRACT

This study presents a hybrid energy harvesting system for Unmanned Aerial Vehicle (UAV), that integrates solar power and hydrogen fuel cells to enhance flight performance. The study commenced with the analysis of the case study UAV flight power design specifications using analytical methods. the estimation of number of solar cells and the hybridization of the solar and hydrogen fuel cells. A Computer Aided Design (CAD) model of the solar cell arrangement is created using industrial software which enables the visualization of the arrangement on the wing in a virtual environment. The mission performance analysis was carried out using Excel tool and Matrix Laboratory (MATLAB). The redesigned system increased available power to 580 Watts with a weight penalty of 1.5 Kg thereby reducing the payload mass from 4.627 kg to 3.085 kg. To assess the structural implications of this result, a stress analysis was performed using Computer-Aided Three-dimensional Interactive Application (CATIA) and Abaqus software which revealed a negligible failure index of 0.000757. The hybrid system achieved a 120% increase in power that extended the endurance from 4.2 hours to 16.3 hours and the range from 6 km to 230 km. The design offers a promising solution for enhanced UAV performance.

1.0 Introduction

The hybrid energy harvesting UAV designed by the 2021/2022 MSc research students at Air Force Institute of Technology was used as the test bed for this paper. The case study UAV has an endurance of about four hours using a combination of a 7S 4000 mAh Li-Po battery and hydrogen fuel cell system as its power source (AFIT-ALTA, 2022). The design goal was to integrate the fuel cell to increase the endurance and range parameters of the UAV, as well as power the onboard electronic or avionics components. The increase in the endurance is significant. However, at instances where there is strong turbulence resisting the motion of the UAV, the endurance calculated for the mission falls short and the liquid hydrogen fuel is not sufficient to accomplish the mission. Therefore, with an appreciable wing geometry, solar cell is selected based on its environmental friendliness and energy conversion efficiency compared to other energy sources to counter this limitation. The solar cells will be sized and arranged in series on the upper surface of the plan form area of the wing to provide an operating voltage higher than the battery voltage to be able to charge the battery and onboard avionic equipment. The solar cells will be arranged to flush with the wing surface in order not to increase drag. Collaterally, integration of the solar cells on to the wing of the UAV is accompanied with some mass complexities which will either increase or decrease the operational empty weight of the UAV. (Saravanakumar *et al*., 2023; Wang *et al*., 2022; Matlock *et al*., 2019). Unmanned Aerial Vehicle (UAV), commonly known as drone is an aircraft without any human pilot or crew onboard. They are controlled remotely with the aid of sensors that transmits and receive radio signals for communication (Mohammadnia *et al*.,2020). The UAV under study, was designed to have an all-up mass of 10 Kg and a wingspan of about 4.2 m. The image of the aircraft is shown in Figure 1. It serves as the case study hybrid energy UAV for flight power performance analysis.

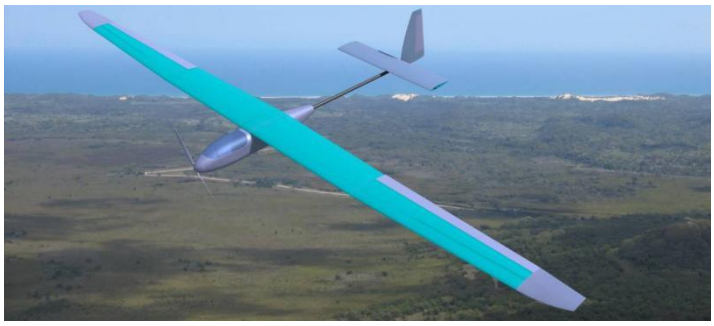

Figure 1: Hydrogen fuel cell UAV (AFIT-ALTA, 2022)

In recent times, UAVs play a major role in global society due to their ability to carry payloads, operate and monitor complex scenarios where the presence of onboard human pilots are needless. UAVs are however constrained by power, which invariably affects their performance during most flight missions. Typically, therefore, the mission profiles of these UAV's are limited by insufficient range and endurance. Its main source of power is either engine or batteries. A hybrid energy harvesting system offers increased flexibility into the UAV design by allowing choice of specific instrument regardless of the electrical bus and to expand the system as system requirement changes. Some of the energy harvesting technologies used to generate electricity for air vehicles include Piezoelectric process, Thermoelectric process, Electromagnetic process and Photovoltaic techniques. The basic components of a conventional energy harvesting system is depicted in Figure1. It includes the energy input source, detection and storage and the loads to which the scavenged energy will be supplied to. Components required to achieve the process include transducers to convert ambient energy to electrical energy, power management circuit to adjust the harvested energy based on the needs of the loads embedded in the UAV and lastly, an energy storage buffer to deliver the high power to the load.

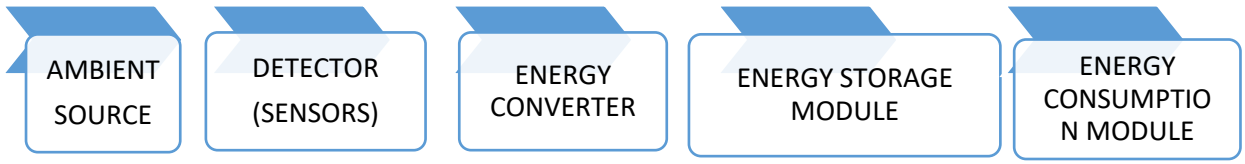

Figure 2: Conventional Energy Harvesting System (Prauzek *et al*., 2018)

Various concepts are employed in the utilization of solar energy, but one of the ways proposed to tap maximum amount of electrical energy efficiently and effectively from the solar is a hybrid combination of solar panels and thermoelectric generators (Mohammadnia *et al*., 2020)

Thermoelectric generator (TEG) is a solid-state device that converts heat energy to electrical power by means of semiconductor charge carriers serving as a working fluid. They function like heat engines but are less massive with no moving parts (Rezania and Rosendahl, 2012). Their advantages are that they do not require any fluid for fuel or cooling, making them non-orientation dependent and allowing for use in zero-gravity or deep-sea applications. In this system the solar produces heat in addition to the photons that are focused onto the panels. The heat energy is tapped and converted into electrical energy to boost the energy produced by the solar panels. Ozbek *et al*., (2021) used a Polymer Electrolyte Membrane (PEM) fuel cell – Li-Po batteries as a hybrid energy harvester to produce more wattage power for the fixed wing UAVs to achieve large endurance. In his experiment, he observed that, approximately 160 – 170W power was met by the fuel cell when no preconditions were applied. The fuel cells converted the chemical energy of the fuel into direct current electricity through electrochemical process without any moving parts (Barbir, 2012). Also made studies into providing some regenerative power from some avionics or electronic components installed in UAVs by equipping it with energy harvesters which can scavenge energy from radio frequency (RF) using relays have been carried out. However, the energy generated is not enough to power large loads. Citroni *et al.* (2019)

therefore proposed a hybrid energy harvesting system that can recover energy from solar and RF energy sources at the same time to significantly improve the energy required for long flights. The RF energy from the surroundings serves as an alternative power source for powering the UAV when there is insufficient or no radiation to generate electrical power from the solar panels. Furthermore, there is the need to consider better aerodynamics properties irrespective of design modifications to increase the overall UAV performance during its flight missions (Wang *et al.*, 2019). The focus of the study therefore includes the analysis and design of takeoff, landing, climb and cruise power supply system and its performance evaluation in terms of the UAV endurance, range and other flight performance indicators.

2. Materials and Methods

2.1 Materials

The aircraft understudied has design specifications as shown in the Table 1.

Table 1: Design specification of case study UAV

Parameters	Values
Design Gross weight	10 kg
Maximum ceiling altitude	10,000 ft.
Maximum range	6 km
Design cruise speed	14.3 m/s
Maximum balanced field length	<100 m
Engine	AXI 4130/20 Electric Motor
Wing area	1.009835 m^2
Wingspan	4.28 m

The main battery power source was augmented with a hydrogen fuel cell stack on a 7S 4000 mAh Li-Po battery.

2.2 Methods

2.2.1 UAV Power Requirement

2.2.1.1 Determination of Take-Off Power Requirement

Power (P) required for the UAV to successfully achieve a complete take-off is estimated using the formula (Malik, 2020).

$$P = Thrust \times Take - off\ velocity\ . \quad (1)$$

Where the thrust (T) is estimated as;

$$T = D + Wsin\gamma \quad (2)$$

Where the climb angle of the aircraft is represented as γ, D is the drag of the UAV and W is the weight of the UAV.

$$D = \frac{1}{2}\rho V_s^2 S[C_{D0} + kC_{Lmax}^2] \quad (3)$$

Also, the free stream velocity is expressed as;

$$V_s = \sqrt{\frac{2W}{\rho S C_{Lmax}}} \quad (4)$$

Therefore, assuming sea level conditions, the density is assumed to be 1.225 kgm^{-3}, and the UAV specification,$C_{Lmax} = 1.38, \rho = 1.225\ kgm^{-3}, W = 10\ kg, S = 1.009835\ m^2$the free stream velocity is estimated using Equation 4 (Clark, 2018).

Power required for the UAV to successfully achieve a complete take-off is therefore estimated using Equation 1, 2,3 and 4, assuming sea level conditions of density 1.225 kgm^{-3}, and taking the $C_L, W\ and\ S$ from the case study UAV specification to first obtain the free stream velocity as follows:

$$C_{Lmax} = 1.38, \rho = 1.225\ kgm^{-3}, W = 10\ kg, S = 1.009835\ m^2$$

$$V_s = \sqrt{\frac{2(10 \times 9.81)}{1.225 \times 1.009835 \times 1.38}} = 10.7205\ ms^{-1}$$

Therefore, the minimum speed at which the UAV can be maintained to generate lift for a successful take-off is estimated to be $10.7205\ ms^{-1}$.

To ensure a safety margin during take-off, a liftoff velocity is also estimated which is about 20% greater than the stall velocity is obtain using Equation 5.

$$V_{LO} = 1.2V_s \quad (5)$$

$V_{LO} = 1.2(10.7205) = 12.8646\ ms^{-s}$

The drag the UAV will be subjected to during take-off is also estimated using Equation 3 to obtain

$$D = \frac{1}{2}(1.225) \times (10.7205)^2 \times (1.009835) \times [0.0109 + 0.0446(1.38)^2 = 6.7464\ N$$

Considering a climb angle of 5 degrees, the Take-off thrust (T) is projected from Equation 2

$$T = 6.7464 + 10(9.81)\sin(5)$$

$$T = 15.2963\ N$$

Therefore, having estimated the value for the take-off thrust and Lift-off velocity, the power required by the UAV for take-off is estimated from Equation 1.

$$P = 15.2963\ \times 12.8646 = 196.7820\ Watts$$

Therefore, the power required to achieve a complete take-off by clearing the 50 feet obstacle height is 197 watts.

2.2.1.2 Determination Climb Power Requirement

For climb performance evaluation (Figure 3), parameters considered are the rate of climb (ROC), and the climb angle (γ). With these parameters well estimated, the UAV will be able to climb at a good rate over vertical obstacles. It is worth noting that, the maximum ROC is experienced at sea level and decreases as the altitude increases. ROC which is defined as the rate of change of altitude per unit time is mathematically expressed as in Equation 6 (Anderson, 2020)

$$ROC = \frac{dh}{dt} = \dot{h} \tag{6}$$

Where h = the altitude and t = time.

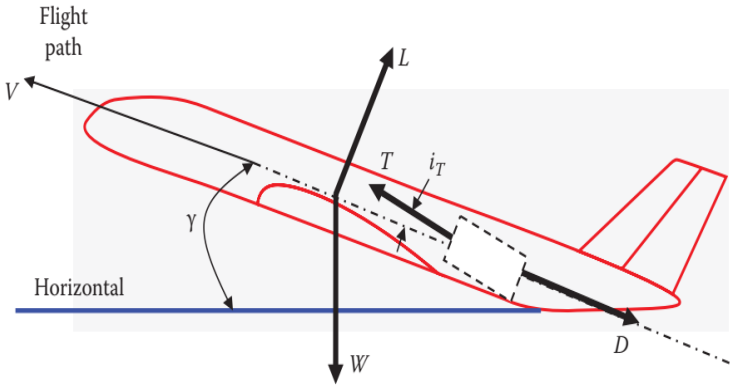

Figure 3: Forces acting on an aircraft in Climb. (Malik, 2020)

The propeller of the UAV is mounted at an angle known as the climb angle (γ) of 5°. Since the UAV will be climbing at a constant acceleration 'a', from Newton's second law, the equilibrium of the forces in the direction of flight can be expressed as in Equation 7;

$$Tcos(i_T + \alpha) - D - Wsin(\gamma) = ma = m\left(\frac{dv}{dt}\right) \tag{7}$$

Where 'i_T' is the angle of incidence, α is the UAV angle of attack.

If all forces are assumed to pass through the center of gravity, i_T and α are also assumed to be zero, then Equation (6) becomes Equation 8 (Anderson, 2020)

$$T - D - mgsin\gamma = m\left(\frac{dv}{dt}\right) \tag{8}$$

The airspeed vector 'V' is then resolved into its vertical and horizontal component. By definition, the vertical component $\dot{h}$ is the ROC of the UAV. From Figure 4, the relationship between the forward speed and ROC is expressed as in Equation 9.

$$Vsin(\gamma) = \frac{dh}{dt} = \dot{h} \tag{9}$$

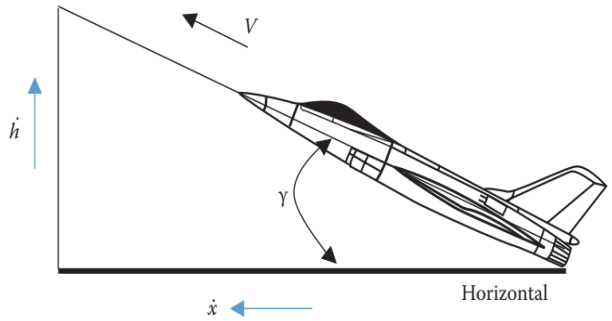

Figure 4: Horizontal and Vertical Airspeed component for ROC

Multiplying Equation (8) by V and substituting it into Equation 9 yields,

$$(T - D)V = \frac{d\left(mgh + \frac{1}{2}mV^2\right)}{dt} \tag{10}$$

Where $(T - D)V = excess\ power\ and\ \ mgh + \frac{1}{2}mV^2 = \ the\ UAV\ total\ energy.$

Therefore, the UAV ROC is estimated using the Equation 11,

$$ROC = \frac{(T-D)V}{W} \tag{11}$$

ROC, the power required for the climb phase is calculated using the Equation 12,

$$P_{climb\ req} = (T - D)V_{lo} \tag{12}$$

From Equation (11),

$$ROC = \frac{[(15.2963 - 6.7464) \times 12.8646]}{10 \times 9.81} = 1.1212\ ms^{-1}$$

The UAV will be climbing at a speed of $1.1212\ ms^{-1}$ to cruise altitude where climbing will stop. This indicates that, ROC generally decreases with altitude to the cruise altitude where it becomes zero. Using the Equation 12, , the power required for the climb phase is

$$P_{climb\ req} = (15.2963 - 6.7464) \times 12.8646 = 109.99\ Watts$$

2.2.1.3 Determination of Cruise Power Requirement

The governing principle in straight and level flight is the Newton's second law of motion which explains how an object's motion changes when a force is applied. The external forces of interest in this flight phase are the UAV weight (W), thrust (T) from the battery, drag (D) and lift (L) as shown in Figure 5.

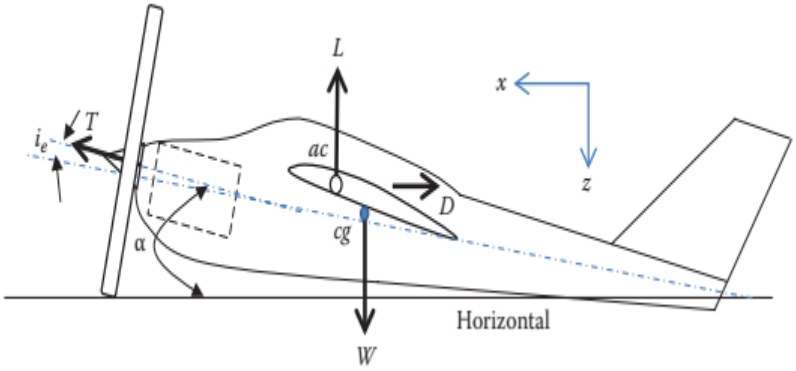

Figure 5: Equilibrium of forces in a straight level flight (Malik, 2020)

In an un-accelerated straight and level flight, the governing Equations 13 of motion are.

$$\sum F_x = 0 \quad and \quad \sum F_z = 0 \tag{13}$$

This is an implication that, the UAV is in a trim or equilibrium state. From figure 5, the trim equations along z and y axes are Equation 14 and Equation 15.

$$D = Tcos(\alpha + i_i) \tag{14}$$

$$W = L + Tsin(\alpha + i_i) \tag{15}$$

where,

α = the angle of attack and

i_i = the engine setting angle.

However, for ease of estimation, the following assumptions are made.

(i) For straight and level flight, UAV angle of attack is assumed to be zero.

(ii) Also, since the UAV has no engine mounted on it, the engine setting angle is also assumed to be zero.

Hence, Equations 14 and 15 becomes.

$$D = T \tag{16}$$

$$W = L \tag{17}$$

Indicating that, for un-accelerated straight and level flight, the conditions in Equations (16).

and (17)are true. Therefore, in a steady level flight, when the available power is more than the required power, the UAV will accelerate and vice versa. The required power is a function of airspeed. To have a steady level flight, the lowest amount of energy is required from the power system and this is achieved at the minimum power speed. However, there will be no steady level flight when the power generated produces a velocity that is less than the minimum required power speed V_{minp}which is generally about 30% of the maximum available power (Clark, 2018). The minimum power speed is estimated using the Equation 18,

$$V_{minP} = \sqrt{\frac{2mg}{\rho S\sqrt{\frac{3C_{D0}}{k}}}} \tag{18}$$

where

ρ = density of the air at the cruise altitude which per the case study specification is 10,000 feet. The air density at 10,000 feet from International Standard Atmosphere (ISA) Table is 0.413 0.413 kg/m³.

Since for this condition, the thrust produced is equal to the drag generated as a result of forward motion, the minimum power required can be estimated using Equation 19,20, 21 and 21.

$$P_{min} = T_{minP} \times V_{minP} = D_{minP} \times V_{minP} \tag{19}$$

$$where \quad D_{minP} = \frac{1}{2}\rho_{10,000}V_{minP}^2 S\left(C_{DO} + kC_{L\,minP}^2\right) \tag{20}$$

$$Also, \quad C_{L(minP)} = \sqrt{\frac{3C_{DO}}{K}} \tag{21}$$

Therefore, substituting equation 21 into Equation 20 yields Equation 22,

$$D_{minP} = 2\rho V_{minP}^2 S C_{DO} \tag{22}$$

Using Equation 18,

$$V_{minP} = \sqrt{\frac{2 \times 10 \times 9.81}{\left[0.413(1.009835)\sqrt{\frac{3(0.0109)}{0.0446}}\right]}} = 10.7716\, ms^{-1}$$

Hence, since the minimum required power velocity for cruise is greater than the stall velocity, it can be concluded confidently that, during steady level flight, the UAV will be able to cruise at the minimum power velocity of $10.7716\, ms^{-1}$ without stalling. With this condition, the thrust produced is equal to the drag generated because of the forward motion, the minimum power required can be estimated using Equation 19,20, 21 and 22 to obtain

$$D_{minP} = 2(0.413)(10.7716)^2(1.009835)(0.0109) = 1.0549\ N$$

Therefore, the minimum power required to sustain the UAV in a steady level flight is calculated from Equation 19 as,

$$P_{\min} = (1.0549) \times 10.7716 = 11.3631\ Watts$$

2.2.1.4 Determination of Descent Power requirement

Here, the velocity will be reducing from the cruise velocity to a new velocity known as the approach velocity until the UAV touches down. The descent procedure is as depicted in Figure 6.

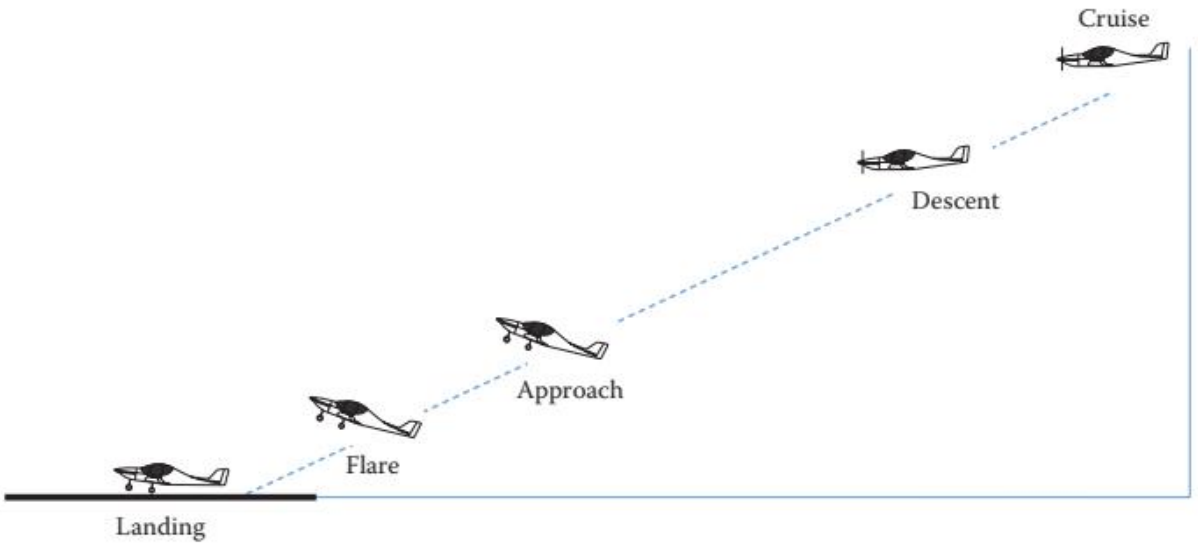

Figure 6: Descent process from Cruise phase of flight (Clark 2018)

Just like the climb phase which the UAV uses a climb angle to climb, the descent also occurs at a constant angle known as the angle of descent (γ). The descent is controlled by varying the power to thrust ratio which is estimated according to (Clark, 2018) to be 10% to 30% of the total power to thrust ratio. However, since the case study UAV is designed to have gliding characteristics due to its wing design, in the absence of power, the UAV will be capable of gliding by taking advantage of the air gradient in a process known as dynamic soaring.

In a descending flight, the drag is greater than the thrust and the lift is smaller than the weight. Therefore, if the approach speed is kept constant, the kinetic energy possessed by the UAV will remain constant while the potential energy will decrease due to loss of altitude.

Assuming the descent angle is the same as the climb angle, the rate of descent (ROD) can be estimated using equation 23,

$$ROD = V_{des} \sin(\gamma) \tag{23}$$

Where, V_{des} is the UAV approach speed and γ is the descent angle.

Descent velocity for UAVs in the weight category of the case study UAV are estimated in the range of 1m/s to 3 m/s. Therefore, assuming a descent velocity of 3 m/s and a descent angle of $5°$ degrees. The ROD is estimated to be,

$$ROD = 3 \sin(5°) = \ \ 0.2615\ ms^{-1}$$

Therefore, the UAV will have a controlled descent rate of 0.2615 m/s until it touches ground and the power gradually reduced to zero for the UAV to go into a complete rest.

Also, assuming a descent thrust of 20% thrust from the cruise thrust at steady level flight, the descent thrust can be estimated as,

$$T_{des} = 20\% \; of \; T_{min} \tag{24}$$

Hence for that of the case study UAV, the descent thrust is calculated from equation 24 to be,

$$T_{des} = \frac{20}{100} \times 1.0549 = 0.211 \; N$$

The power required for descent flight is therefore estimated using the expression (equation 25),

$$P_{des} = T_{des} \times V_{des} \tag{25}$$

$$P_{des} = 0.211 \times 3 = 0.6329 \; Watts$$

The power required for the UAV to descend and subsequently land is 0.6329 Watts.

2.2.1.5 Landing

Landing is the final phase of flight. This phase encompasses the ability of the UAV to safely land on the ground and gradually come to a complete stop prior to a controlled descent. It is the opposite to the take-off performance. Unlike the take-off where the required power is large, landing requires minimum or no power to execute this phase. However, it must be controlled in order not to cause destruction to the structural or avionics components. During descent and landing, the power consumed is generally less compared to take-off and climb phase. MATLAB codes were generated for the performance estimations.

2.2.2 Power Supply

To provide the needed power as determined, harnessing of renewable energy from the surrounding environment - solar energy in combination with the installed hydrogen fuel cell is proposed. The UAV will therefore harvest additional energy from the photovoltaic cells spread on its wingspan as well as from the hydrogen fuel cell which converts liquid hydrogen into electrical power via an electrochemical process. The proposed hybrid combination model of the solar cell system and the hydrogen fuel cell system is shown in Figure 7.

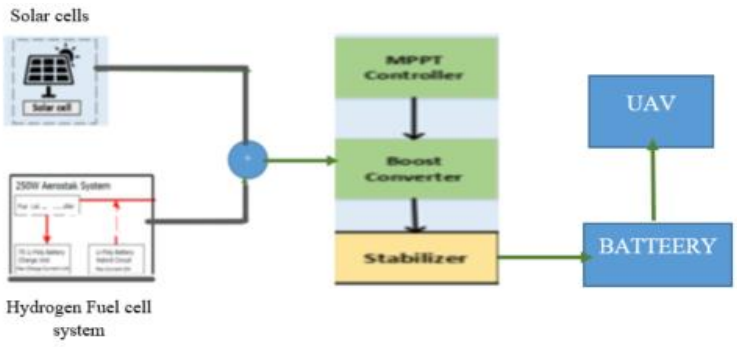

Figure 7: Proposed Hybrid Energy Harvesting System

2.2.2.1 Solar Energy

The photovoltaic cell selected is the monocrystalline solar cell made from a single silicon crystal. Though they are more expensive, they have a higher conversion efficiency rating ranging between 15% to 25%. In other words, they have the ability of converting about 25% of the sunlight absorbed into usable energy (electricity). A monocrystalline solar cell has greater longevity of about 40 years and also characterized by lower

temperature coefficient which makes it more efficient under heat (Yadav *et al*., 2019). Figure 8 represents a pictorial view of the monocrystalline solar cells panel.

Figure 8: Monocrystalline solar cell.

Table 3: Photo voltaic cell specification (Monocrystalline)

Parameter	Specification
Mass of solar cell	4 gm
Length and width	78 mm by 77 mm
Efficiency of solar cell	18.6%
Rated voltage	0.5 V or 0.6 V
Rated current	2.1 A

The number of solar cells and its arrangement on the Wing are therefore estimated according to the power need of the UAV with respect to the specification given in Table 1.

2.2.2.1.1 Determination solar charge capacity

The determination of charge capacity as per the specification of the selected PV cell (Table 3) of which 0.5 V is produced from, requires a combination of cells in series to be able to generate the required voltage that can continuously charge the Li-Po battery with a constant voltage of 22.2 V. Therefore, to obtain the 22.2 V, the number of cells required is estimated to be:

$$\frac{22.2}{0.5} = 44.4\ cells\ approximately\ 45\ PV\ cells.$$

However, due to different type of losses that will be encountered in the course of conversion there is the need to add about 35% more cells to get a voltage above the constant voltage charge of the battery, and since the wing planform area and the span are fixed as per the case study UAV, the cells will be arranged on the planform in a way that will not disrupt the boundary flow. Hence, the estimated number of cells to be used for the generation is,

$$45 \times 0.35 \cong 15 \text{ more cells.}$$

Hence, total number of PV cells are, $45 + 15 = 60$ PV cells.

Therefore, the ideal total voltage acquired from the solar cells will be,

$$60 \times 0.5V = 30V$$

Ideal watt power for the solar cells is expressed as

$$P_{solar} = V_{solar} \times I \quad (26)$$

Where I is the rated current capacity of the PV cell and V_{solar} is the total voltage acquired from the combination of the PV cells. Hence, estimating the solar power from Equation 26 gives.

$$P_{solar} = 30\ V \times 2.1\ A = 63\ Watts$$

Ideally, the solar cells should produce whatever watts of electricity under perfect conditions. But practically, the peak sunshine hours depending on the climatic condition in the region to which the UAV will be operating is factored in the estimation. This makes the output power vary. Hence, solar output power per day is estimated as 75% of the total output capacity. Other losses are considered to be 25%. Assuming a 7-hour sunshine in the northern part of Nigeria, the solar output power will be calculated as;

$$solar\ power\ output = solar\ power\ rating \times number\ of\ peak\ solar\ hours \times 75\%$$

$$P_{solar\ output} = P_{solar} \times Peak\ solar\ hours \times 75\% \quad (27)$$

Therefore, from Equation 27, the solar power is computed as;

$$Solar\ power\ output = 63W \times 7hr \times 0.75$$

$$= 330.75\ \ Watt - hour\ (Wh)$$

Hence, converting the watt-hour to Ampere-hour using Equation 28 yields.

$$Solar\ Amp - Hr = \frac{Watt-hour}{total\ solar\ voltage} \quad (28)$$

$$Solar\ Amp - Hr = \frac{330.75}{30} = 11.25\ Ahr$$

2.2.2.1.2 Determination cells arrangement on wing plan form

Examining the size and shape of the wing of the UAV under consideration, the solar cells is divided into two and arranged on the plan form of the wing taking into consideration the dimension of each cell. The plan form area and span of the wing are $0.9724m^2$ and $4.2m$ respectively. Wing is tapered from root to tip. Figure 9. represents the wing under consideration.

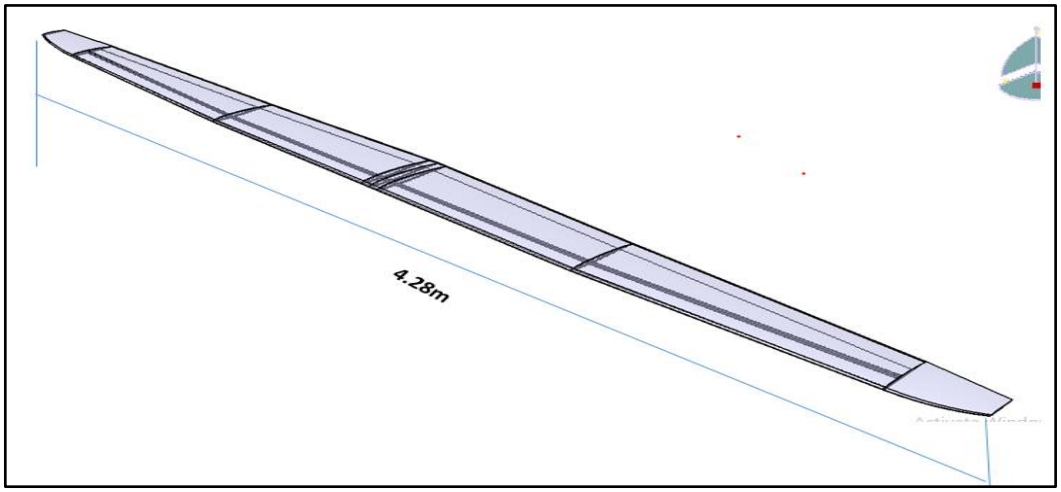

Figure 9: Wing geometry of case study UAV

Table 4: Wing specifications (AFIT- ALTA 2022)

Parameter	Specification
Span	4.42 m
Aspect ratio (AR)	18.14
MAC	0.2418 m
Max coefficient of lift	1.38

The solar cells are rectangular in shape due to their dimension which is $78\ mm \times 77\ mm$ in terms of length and width to give:

$$78\ mm \times 77\ mm = 0.078\ m \times 0.077\ m$$

$$Area\ of\ PV\ cell\ is\ 6.006 \times 10^{-3} m^2$$

Therefore, as per the estimation, a total of 60 solar cells will be housed on the wing surface of the UAV, covering about 0.3604 square meter which is about 36% of the wing area. Figure 10 shows how the cells are arranged and wired in series to obtain the desired voltage output of 30 volts. The solar cells will be augmented with a Maximum Power Point Tracking solar charger (MPPT) to ensure that, the loads receive maximum current to be used by quickly charging the Li-Po battery and also powering the onboard avionic equipment.

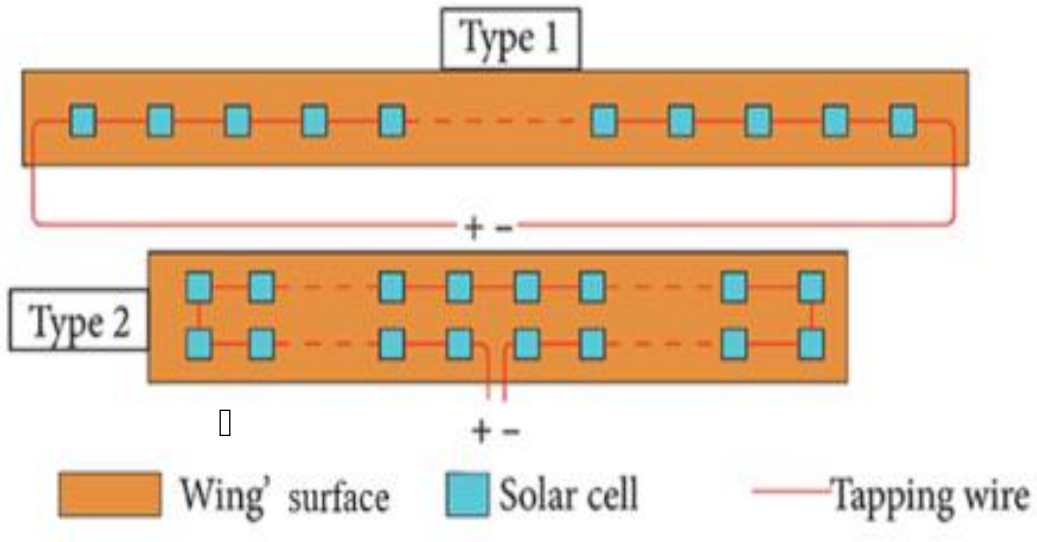

Figure 10: Arrangement and wiring of solar cells on wing surface

The CAD model of the solar cell arrangement is created using industrial software which enables the visualization of the arrangement in a virtual environment. The arrangement is made up of multiple solar cells that are connected in series for the desired voltage and current output. Additionally, a robust support structure is designed to hold the solar cells firmly on the wing. This support is transparent enough to allow the cells capture maximum sunlight from the surrounding environment. Figure 11 shows the CAD model of the arrangement of solar cells on the wing planform area of the case study UAV

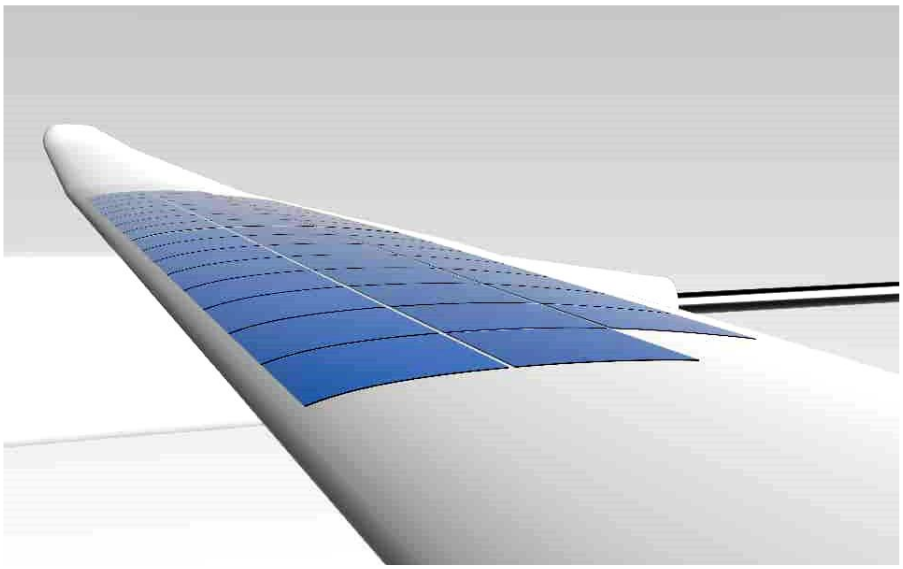

Figure 11: Arrangement and wiring of solar cells on wing surface

2.2.2.2 Hydrogen Fuel Cell System

This system is capable of generating electricity through an electrochemical reaction between hydrogen and oxygen which gives off heat and water as by-products. They are clean form of energy with no carbon dioxide emissions or air pollutants that may lead to health issues in humans. They consist of anode, cathode and electrolyte membrane for its operation. When hydrogen passes through the anode, a catalyst splits the hydrogen molecule into protons and electrons. The protons pass through the electrolyte membrane whereas the electrons are forced through a circuit, generating an electric current and excess heat.

The hydrogen fuel cell specification for the case study UAV, has the specification shown in Table 5 while Figure 12 is the pictorial view of the hydrogen fuel cell used in the design of the case study UAV. ((AFIT- ALTA 2022).

Table 5: Hydrogen fuel cell specification

H3 Dynamics AEROSTACK A-250	
Rated Power (FC)	250 W
Voltage	24.5-35.2 V
Specific Power	347 W/Kg
Start Up time	< 20 s

Figure 12: Hydrogen fuel cell

2.2.2.3 Hybridization of Solar and Hydrogen Fuel Cells

The hybrid combination model of the solar cell system and the hydrogen fuel cell system is shown in Figure 13.

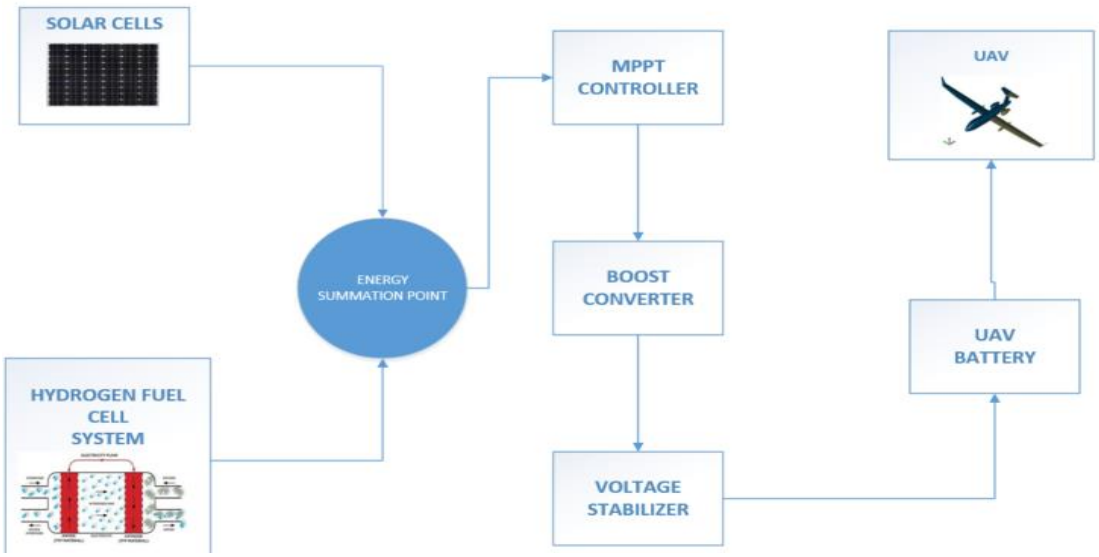

Figure 13: Proposed Hybrid Energy Harvesting System

Total number of solar cells to be employed in the design is 60. Therefore, combining the two generative systems, the total power that is generated from the hybrid energy system of solar, hydrogen fuel cell and the LiPo battery is obtained using equation 29;

$$Total\ voltage = Voltage_{solar} + Voltage_{hydrogen\ fuel\ cell} + Voltage_{LiPo\ battery} \quad (29)$$

$$Total\ voltage = \ 30V + 30V + 22.2V = 82.2\ Volts$$

Considering the weight of each photovoltaic (PV) cell to be 4g, the total weight of the PV cells on the wing surface is therefore estimated to be 240g. In addition, the weight of the maximum power point tracking system (MPPT) to be installed on the fuselage is 1.3 Kg. The above modifications will add to the power requirement of the UAV and therefore forms part of the flight power performance analysis.

2.2.4 Stress Analysis of Wing

To confirm that the wing will not fail when the solar cells are placed on its planform, stress analysis was performed on the wing in order to establish the failure index using CATIA and Abaqus software. The CAD model of the wing was developed in CATIA and imported into Abaqus. Material properties were defined, boundary conditions set and load was carefully applied at the selected area. The model was then meshed and analysis ran to see the visual effect. The Tsai-Hill failure criteria was considered for the failure analysis. The criterion considers the interaction between different stress components and its failure mode. When the failure index of the material is 1, it implies the material has reached its maximum strength and can no longer withstand additional stress.

2.2.5 Flight Performance Analysis

The aim of the study is to enhance flight performance of the AFIT Post Graduate UAV both in endurance and range by designing an enhanced hybrid energy source that meet its mission profile within the constraints of extraneous factors such as environmental conditions and flight altitude. Performance of an aircraft denotes its characteristics and capabilities at various phases of flight. It encompasses a range of factors such as speed, range, climb rate, maneuverability, take-off and landing distances, payload and fuel efficiency. Therefore, understanding and optimizing aircraft performance is critical for guaranteeing a safe and efficient flight operations, as well as achieving specific mission objectives for different types of aircrafts (Anderson, 2010). MATLAB codes were generated for the performance estimations.

2.2.5.1 Endurance

According to (Traub, 2011), for electric powered UAVs, the maximum endurance is estimated using the relation for minimum power and thrust. The condition for maximum endurance is given by Equation 30,

$$C_{D0} = \frac{1}{3} k C_{L\,minP}^2 \quad (30)$$

Hence, the maximum endurance is estimated using the Equation 31,

$$E_{max} = Rt^{1-n} \left(\frac{\eta_{tot} V \times C}{\left(\frac{2}{\sqrt{\rho S}}\right) C_{D0}^{\frac{1}{4}} \left(2W\sqrt{\frac{k}{3}}\right)^{\frac{3}{2}}} \right)^n Hours \quad (31)$$

$$C_{D0}\ condition\ for\ the\ case\ study\ is, \qquad C_{D0} = \frac{1}{3}(0.0446)(0.8563)^2 = 0.0109$$

where $\boldsymbol{Rt}$ = the power system hour rating in hours which is assumed to be 1 hour since the discharge time over which small rechargeable battery packs are rated is typically per hour,

V = the power system total voltage, **C**= the energy source capacity in ampere hours,

$\boldsymbol{\eta_{tot}}$ = the total efficiency due to losses in the propulsion system which consist of propeller efficiency, servo motors etc. It is assumed to be 0.8 and **n** = a discharge parameter which is dependent on the battery type and temperature. Traub (2011) investigated the impact of discharge rate on effective battery capacity by simulating an ideal battery: no Peuket effect using n=1 and n=1.3 (typical for Lithium polymer batteries).

2.2.5.2 Range

Range is an essential performance that determines how far the UAV can fly with its available battery power. This is the maximum distance an aircraft can travel with a full load of fuel tank. However, in the case of UAVs, it is the distance the UAV can travel with its available electric power. Flight range of UAVs in the weight class of 10 Kg can vary significantly depending on the design and purpose of the UAV. Generally, UAVs within this weight class might have flight ranges of around 10 to 50 kilometers on a single battery charge.

The range is easily estimated (equation 32) after obtaining the endurance by,

$R=E\times U_R$ (32)

Where R = range

E = endurance

U_R= required flight velocity for maximum range of the UAV – equation 33.

$$U_R = \sqrt{\frac{2W}{\rho S}\sqrt{\frac{k}{C_{D0}}}} \quad (33)$$

However, since the design cruise velocity was given as part of the specification as $14.3\ ms^{-1}$, it is used to compute the range to meet the mission profile of the UAV.

3. Results and Discussion

3.1 Power Requirement

Power required for the UAV to successfully achieve a complete take-off is estimated using equation 1, 2, 3 and 4 as given in section 2, assuming sea level conditions of density 1.225 kgm^{-3}, and taking the $\mathrm{C_L}, \mathrm{W}$ and S from the case study UAV specification to first obtain the free stream velocity. Therefore, the power required to achieve a complete take-off by clearing the 50 feet obstacle height is 197 watts. The power required for the climb phase is calculated using the equation 13, to obtain 109.99 Watts. For the Cruise Power Requirementthe minimum power required is estimated using equations 18,19, 20 and 21 to obtain $\mathrm{D_{minP}} = 1.0549\ \mathrm{N}$. Hence, the minimum power required to sustain the UAV in a steady level flight is calculated from equation 18 to obtain $\mathrm{P_{min}} = 11.3631$ Watts. Descent power requirement using the descent velocity for UAVs in the weight category of the case study UAV are estimated in the range of 1m/s to 3 m/s. Therefore, assuming a descent velocity of 3 m/s and a descent angle of $5°$ degrees the ROD is estimated from Equation 22 to be $0.2615\ \mathrm{ms}^{-1}$. Therefore, the power required for the UAV to descend and subsequently land is 0.6329 Watts. The power required for various flight phases are presented in Table 6 and depicted in Figure 14.

Table 6: Power requirement

Flight Phases	Power Required (Watts)
Take-Off	197
Cruise	11.3631
Descent	0.6329

Landing is the final phase of flight. This phase encompasses the ability of the UAV to safely land on the ground and gradually come to a complete stop prior to a controlled descent. It is the opposite to the take-off performance. Unlike the take-off where the required power is large, landing requires minimum or no power to execute this phase. However, it must be controlled in order not to cause destruction to the structural or avionics components. During descent and landing, the power consumed is generally less compared to take-off and climb phase.

3.2 Battery Capacity

The energy consumed at the various stages of flight varies significantly depending on the size of the UAV, design, payload, the mission requirement, and environmental factors. Considering the critical phases under study which includes take-off, climb and cruise, the individual power consumed at these phases for the case study UAV, are indicated on the mission profile in Figure 14.

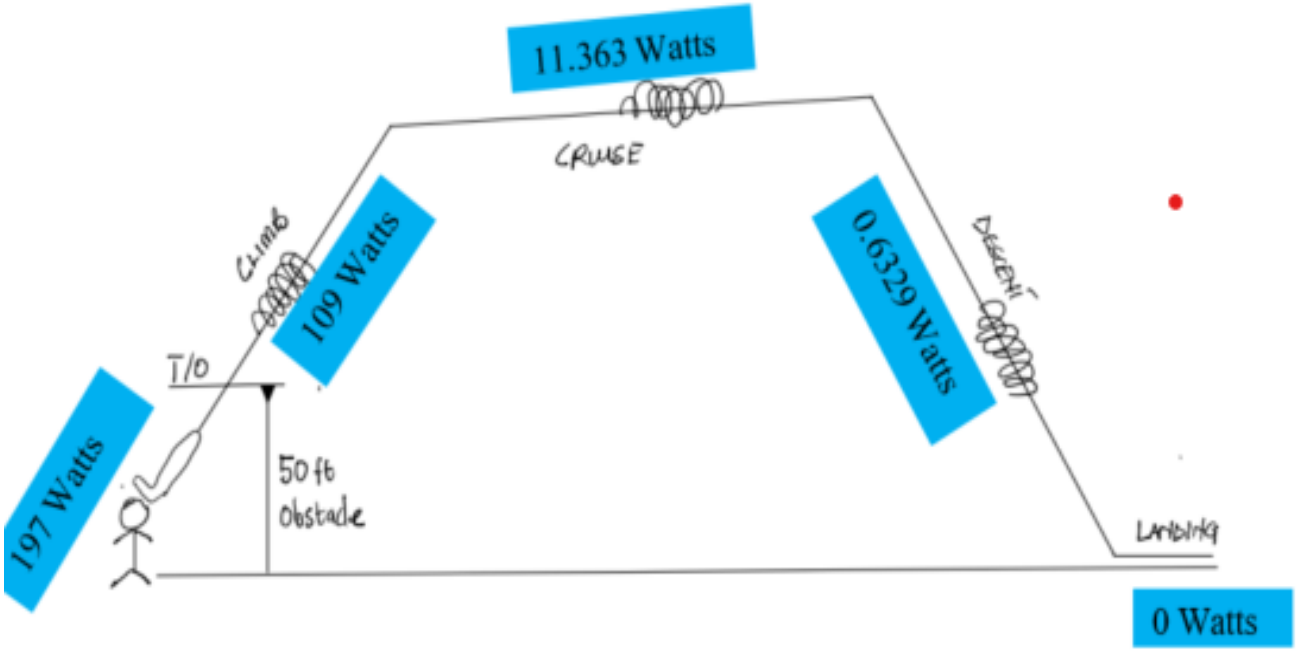

Figure 14: Mission profile of power required at various phases of flight.

From Figure 14, take-off requires a significant amount of power- 17 Watt since the UAV needs to reach a sufficient altitude and velocity to maintain a stable flight. The climb phase is the second largest power (109 Watt) consuming phase of the profile since the UAV continues to use a significant amount of power to reach its desired cruising altitude. Next energy consuming phase is the Cruise phase. The power consumption- 11.363 Watt at this phase is stable as the UAV maintains a constant speed and altitude throughout this phase. During descent (0.6329 Watt) and landing, the power consumed is generally less compared to take-off and climb phase. It is therefore obvious from Figure 14 that the battery must deliver a minimum power of 197 Watts attributable to the takeoff phase to achieve the mission profile of the UAV.

3.2 Flight Performance Analysis

The flight power performance of an aircraft encompasses a range of factors such as speed, range, endurance, climb rate, maneuverability, take-off and landing distances, payload, and fuel efficiency- greater speed using less fuel (thrust specific fuel consumption- TSFC), weight and balance.

3.2.1 Endurance

Traub, (2011) investigated the impact of discharge rate on effective battery capacity by simulating an ideal battery: no Peuket effect using n=1 and n=1.3 (typical for Lithium polymer batteries)

$$E_{max} = 1^{-0.3}\left(\frac{0.8 \times 82.2 \times 15.23}{\left(\frac{2}{\sqrt{(0.413)(1.009835)}}\right)(0.0109)^{\frac{1}{4}}\left(2 \times 98.1\left(\sqrt{\frac{0.0446}{3}}\right)\right)^{\frac{3}{2}}}\right)^{1.3}$$

$$E_{max} = 16.286\ hours$$

Therefore, the maximum endurance that the UAV can go within the permissible assumption made for the solar cells receiving solar energy for seven hours continuous is 16.286 hours for the design weight without payload onboard and 9.025 hours with the design maximum mass. However, since it is also on solar power, the UAV will constantly receive power until the solar radiance reduces in energy when the cells can no longer produce enough energy for continuous power supply. When it happens this way, the hydrogen cell system takes over the power supply chain. This is achieved via a power management system. Hence, for this system it can be concluded that, the UAV will have unlimited endurance provided there is sufficient sunlight available for the PV cells to convert into electrical energy. In the absence of sufficient sunshine, the hydrogen fuel system will power the UAV especially during night operations for about 4 hours to its destination before landing.

3.2.2 Range

The range is estimated to be (Equation 32),

$$R = 16.286 \times 14.3 = 232.891\ km$$

The range of the UAV will be more than the estimated range provided there is more than 7 hours' sunlight on the PV cells. However, in the absence of solar power, the UAV will fly for a maximum range of 7.4687 km at a cruise speed of 14.3 meters per second according to initial specification (Table 1).

3.3 Flight Power Analysis

The total power capacity that will be generated from both the battery and the solar cells is 11.25 Ah. This will have tremendous boost in the power efficiency of the UAV and also improves it flight endurance and operational capabilities. Despite the challenges of other factors such as environmental conditions and flight altitude, there will be enough power to compensate to overcome such conditions. Power from the solar cells, however, will not be readily available until approximately 7:30 am due to the assumptions made in the estimation (section 2). The battery and the hydrogen fuel cell will provide power within this early hour. Therefore, their power need is distributed between the generating systems during the flight periods with the aid of a power management system. Figure 15 illustrates a graph of power available against power required at various flight phases of the mission profile of the UAV.

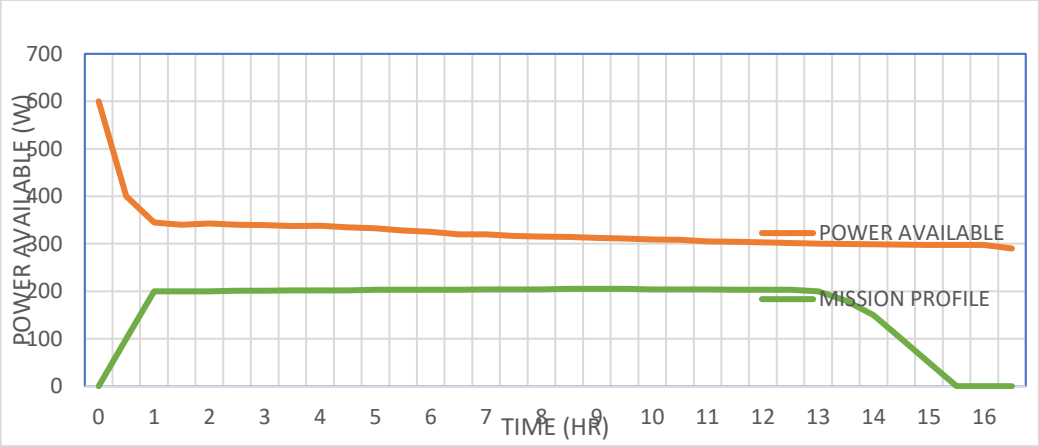

Figure 15: Power available Versus Power required.

After a successful take-off and climb to the maximum altitude, the total available power from the hybrid harvesting system drops from 580 Watts to about 350 Watts. After that big drop, there is a gradual decrease of power within the cruise phase from 350 to 300 Watts. The drop is not as large compared to the drop during the take-off and climb phase. This is because, minimum power is required at the cruise phase of the mission. All things being equal, the power drop remains constant till the end of the flight mission. This is because of the regenerative process of the harvesting system. Figure 16 also shows how the available power generated from the hybrid combination is depleted over the total flight endurance. The power reduces gradually in the mission over time from take-off to landing.

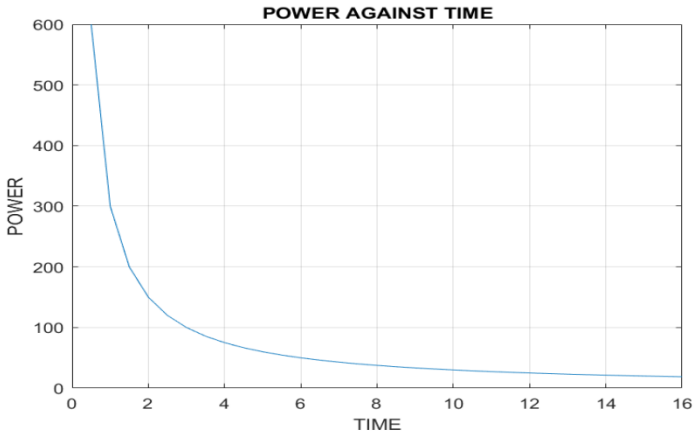

Figure 16: Graph of power against time

3.4 Stress Analysis of Wing

To confirm that the wing will not fail when the solar cells are placed on its planform, stress analysis was performed on the wing in order to establish the failure index using CATIA and Abaqus software. The CAD model of the wing was developed in CATIA and imported into Abaqus. Material properties were defined, boundary conditions set and load was carefully applied at the selected area. The model was then meshed and analysis ran to see the visual effect. The Tsai-Hill failure criteria was considered for the failure analysis. The criterion considers the interaction between different stress components and its failure mode. When the failure index of the material is 1, it implies the material has reached its maximum strength and can no longer withstand additional stress.

3.4.1 Weight Analysis

Under the design constraints on payload due to size, weight and power (SWaP) of both small and micro-UAVs the change in the energy system of the proposed concept led to an increase in the design weight from 5.373 Kg to 6.915 Kg. thereby reducing the maximum payload of the original design by 1.542 Kg. Table 7 shows the various weights of the case study UAV design and the new design.

Table 7: Weight comparison of old and new model of UAV

Parameters	Old design	New design
Design weight	5.373 Ks	6.915 Kg
Payload	4.625 Kg	3.085 Kg
Power to weight ratio	2.497 W/N	5.912 W/N

Furthermore, the power to weight ratio is estimated (equation 34) for both designs and compared, to ensure that the new design with the new hybrid energy method meet the requirements for the intended use of the UAV.

$$Power\ to\ Weight\ raio = \frac{Power\ output\ from\ energy\ system}{Weight\ of\ UAV} \quad (34)$$

The power to weight ratio of both designs is far greater than 1 with the proposed hybrid solar system at 5.9 as against 2.5 of the case UAV. This is an indication that, the UAV will have more power available per unit of weight which can result in better performance capabilities. The P/W ratio of the new design is therefore over 100% greater than the P/W ratio of the original design. This gives room for an increase in the payload mass of the UAV. However, this must be done cautiously without compromising other performance parameters.

3.4.2 Wing Stress Analysis

The maximum stress that can cause the wing to fail at the root was recorded as 0.39 MPa with a wing failure index of 0.000757. The failure index for a material to fail according to Tsia-Hill criteria is 1. Therefore, having a failure index of 0.000757 indicates that, the pressure loads imposed by the solar cells on wing planform will not cause failure of the wing during it operations. Deflection is very small and has little or no significant impact on the wing. Figures 17 to 19 illustrate the CAD drawings of the wing stress analysis.

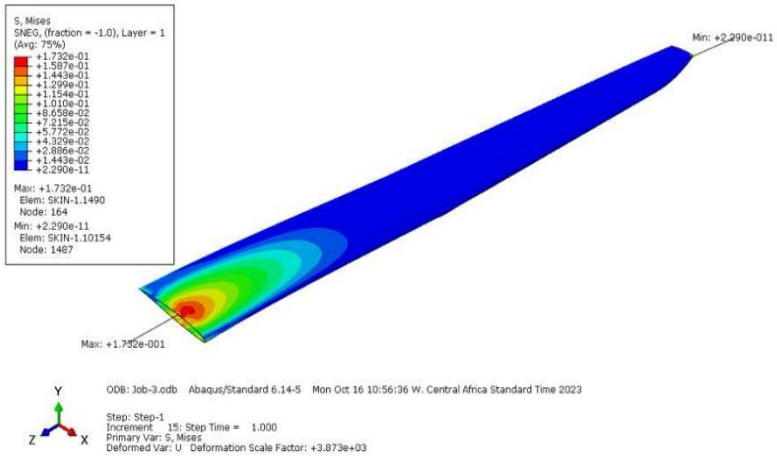

Figure 17: Stress analysis of the wing of case study UAV

Figure 18 shows the stress analysis of the UAV wing. A boundary condition was set at the root section of the wing and pressure loads applied to portions of the wing (Figure 18). A maximum stress of 0.173 MPa was experienced at the root end. This is less than the allowable stress of the composite material used for the wing design, which is 42.27 MPa.

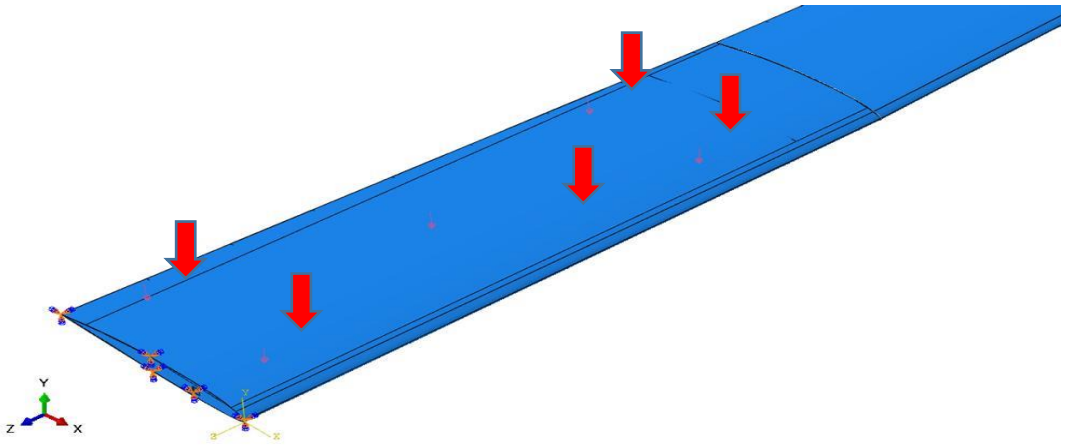

Figure 181: Application of pressure loads of solar cells on planform area.

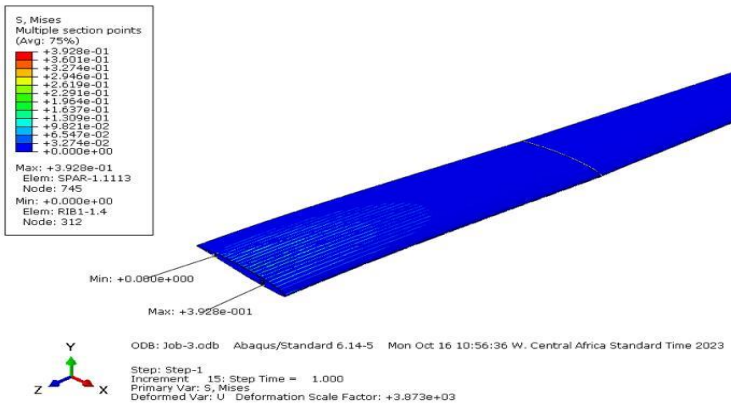

Figure 19: Stress analysis of wing mounted with solar cells.

Figure 19 represents the stress analysis on the wing with the solar cells installed on its planform. From the analysis it was observed that, the maximum stress of 0.39 MPa occurs at the root end of the wing. The area where the cells are concentrated recorded a stress of 0.032 MPa.

3.5 CAD model of the converted UAV with Solar Panel

Figure 20 represents a CAD conversion model with the hybrid solar, hydrogen fuel cells energy system mounted. Performance analysis was carried out based on the mission profile of the UAV and compared to other UAVs in the same class including the case study UAV. Some of the findings made with regards to the case study UAV were that, with the amount of power generated, by the harvesting system, the endurance and range of the UAV increased to 16.3 hours and 232.9 Km respectively.

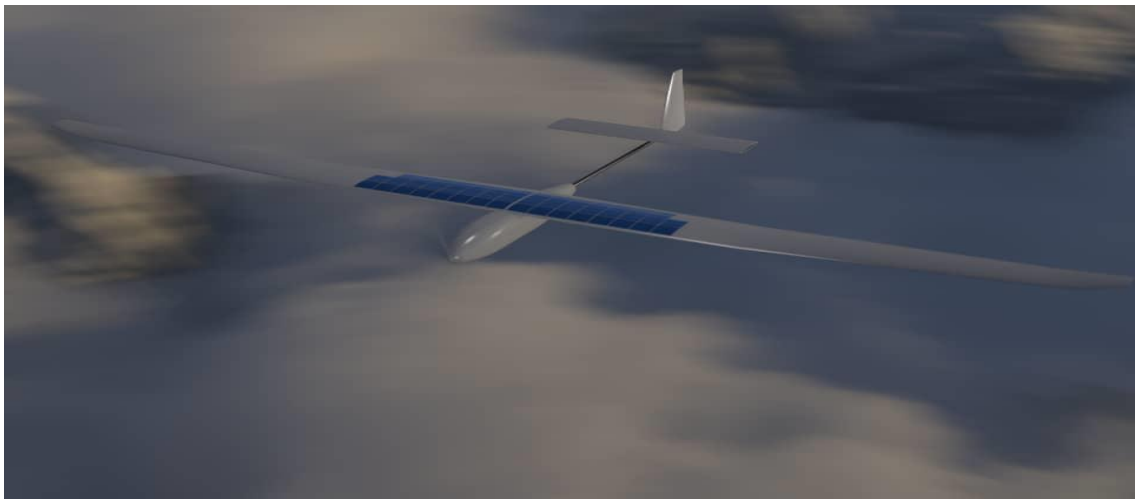

Figure 202: CAD model of the converted UAV with Solar Panel

4. Conclusion

The Unmanned Aerial Vehicle (UAV) was initially designed with a specified endurance of 4.2 hours and a range of 6 kilometres, powered by a 245-Watt output system. However, the integration of the proposed harvesting model significantly enhanced the performance, generating an output power of 580 Watts based on 7 hours of sunshine. Subsequent performance analysis, tailored to the UAV's mission profile, revealed substantial improvements:

1. Endurance increased by 287% to 16.3 hours
2. Range extended by 3765% to 232.9 kilometres

While these enhancements came with a 1.5-kilogram weight penalty, reducing the payload mass from 4.627 kilograms to 3.085 kilograms, stress analysis conducted on the wing using CATIA and Abaqus software ensured the structural integrity of the design. The resulting failure index of 0.000757 confirms the wing's ability to

withstand the added load of the solar cells without compromising its performance. However, considering the evolving landscape of UAV design, with increasing demands for larger payloads and higher altitudes, it is essential to explore additional aerodynamic optimizations beyond power system modifications to further enhance overall UAV performance during flight missions (Wang *et al.,* 2020). Despite the success recorded based on the results presented and discussed, some limitations were observed that needs to be considered in future works on the study. Future work can consider embedding the PV cells into the wing during the wing design phase so that it will flush smoothly with the wing in order to reduce the zero lift drag that will be generated due to the UAV movement.

- Experimental validation of the CAD models can be pursued to validate its accuracy.
- Computational Fluid Dynamics (CFD) analysis can be conducted to ascertain the flow around the wing of the UAV.

References

AFIT- ALTA 2022. AFIT Light Trainer Aircraft Project in ALTA Specification Document. Air Force Institute of Technology, Kaduna, Nigeria.

Anderson, J. 2020. Aircraft Performance and Design. Tata McGraw-Hill Edition, New Delhi.

Barbir, F. 2012. PEM fuel cells: theory and practice. Elsevier Academic Press., London, pp. 44.

Clark, P. 2018. Aircraft performance. In Buying the Big Jets. Fleet Planning for Airlines Taylor and Francis Group Routledge, New Delhi.

Citroni, R., Di Paolo, F. and Livreri, P. 2019. A Novel Energy Harvester for Powering Small UAVs: Performance Analysis, Model Validation and Flight Results. Sensors, 19(8): 5–10.

Malik Y. 2020. Flight Theory and Aerodynamics. Random Publications, New Delhi, India.

Matlock, J., Warwick, S., Sharikov, P., Richards, J. and Suleman, A. 2019. Evaluation of energy efficient propulsion technologies for unmanned aerial vehicles. Transactions of the Canadian Society for Mechanical Engineering, 43(4): 481-489.

Mohammadnia, A., Rezania, A., Ziapour, BM., Sedaghati, F. and Rosendahl, L. 2020. Hybrid energy harvesting system to maximize power generation from solar energy. Energy Conversion and Management, 205: 112352.

Ozbek, E., Yalin, G., Karaoglan, MU., Ekici, S., Colpan, CO. and Karakoc, TH. 2021. Architecture design and performance analysis of a hybrid hydrogen fuel cell system for unmanned aerial vehicle. International Journal of Hydrogen Energy, 46(30): 16453–16464.

Prauzek, M., Konecny, J., Borova, M., Janosova, K., Hlavica, J. and Musilek, P. 2018 Energy Harvesting Sources, Storage Devices and System Topologies for Environmental Wireless Sensor Networks: A Review. Sensors, 18: 2446.

Razykov, TM., Ferekides, CS., Morel, D., Stefanakos, E., Ullal, HS. and Upadhyaya, HM. 2011. Solar photovoltaic electricity: Status and Future prospects. Solar Energy, 85(8): 1580–1608.

Rezania, A. and Rosendahl, LA. 2012. Thermal effect of a thermoelectric generator on parallel microchannel heat sink. Energy, 37(1): 220–227.

Saravanakumar, Y.N., Sultan, MTH., Shahar, FS., Giernacki, W., Łukaszewicz, A., Nowakowski, M., Holovatyy, A. and Stępień, S. 2023. Power Sources for Unmanned Aerial Vehicles: A State-of-the-Art. Applied Science, 13: 11932.

Traub, LW. 2011. Range and Endurance Estimate for Battery-Powered Aircraft. Journal of Aircraft, 48(2): 703–707. https://doi.org/10.2514/1.C031027Prescott Arizona 86301

Wang, Y., Cao, Y., Zhu, C. and Li, Q. 2019. A Method of Reducing Flight Delay by Exploring Internal Mechanism of Flight Delays. Journal of Advanced Transportation, 2019(5): 22–25.

Wang, Y., Kumar, L., Raja, V., AL-bonsrulah, HAZ., Kulandaiyappan, NK., Amirtharaj Tharmendra, A., Marimuthu, N. and Al-Bahrani, M. 2022. Design and Innovative Integrated Engineering Approaches Based Investigation of Hybrid Renewable Energized Drone for Long Endurance Applications. Sustainability, 14: 16173.

Yadav, K., Kumar, A., Sastry, OS. and Wandhare, R. 2019. Solar Photovoltaics Pumps Operating Head Selection for Optimum Efficiency. Renewable Energy, 134: 169-177.